ERRATA

NASA Technical Memorandum 4354

Practical Theories for Service Life Prediction of Critical Aerospace Structural Components

William L. Ko, Richard C. Monaghan, and Raymond H. Jackson

March 1992

Figures 3, 8, and 9 of NASA Technical Memorandum 4354 have been corrected. Please substitute the enclosed corrected pages 17/18 and 21/22 in the report.

NASA Technical Memorandum 4354

Practical Theories for Service Life Prediction of Critical Aerospace Structural Components

William L. Ko, Richard C. Monaghan,
and Raymond H. Jackson

MARCH 1992

NASA

NASA Technical Memorandum 4354

Practical Theories for Service Life Prediction of Critical Aerospace Structural Components

William L. Ko, Richard C. Monaghan,
and Raymond H. Jackson
Dryden Flight Research Facility
Edwards, California

National Aeronautics and
Space Administration

Office of Management

Scientific and Technical
Information Program

1992

CONTENTS

ABSTRACT

A new second-order theory was developed for predicting the service lives of aerospace structural components. The predictions based on this new theory were compared with those based on the Ko first-order theory and the classical theory of service life predictions. The new theory gives very accurate service life predictions. An equivalent constant-amplitude stress cycles method was proposed for representing the random load spectrum for crack growth calculations. This method predicts the most conservative service life. The proposed use of minimum detectable crack size, instead of proof load established crack size as an initial crack size for crack growth calculations, could give more a realistic service life.

INTRODUCTION

Service life (or the number of flights permitted within the proof load interval) of an aerospace vehicle is governed by the individual service lives of critical structural components (for example, NASA B-52 carrier aircraft air-launching-system hooks (ref. 1)). The following procedure describes the conventional method of estimating the service life of critical structural components.

First, a proof load test (which covers all critical flight maneuver loading conditions) is conducted on the critical structural components to load those components up to design-limit load levels. If the proof load test should cause destruction on certain components, then those failed components are immediately replaced, and another proof load test is repeated. If all the structural components should survive the new proof load test, then fracture mechanics is used to theoretically determine the initial "fictitious" (nonexistent) crack size, a_c^p, (critical or incipient crack size associated with the proof load level) at the critical stress point (the location of which is determined from stress analysis) of each structural component. Then, the service life for each structural component is estimated from the amount of crack growth permitted for the initial "fictitious" crack a_c^p to grow and reach the operational limit crack size $a_c^o(a_c^o > a_c^p)$ which is also fictitious, and is calculated from fracture mechanics based on the operational peak load, which is much lower than the proof load. Thus, the amount of available crack growth $a_c^o - a_c^p$ will determine the number of flights available for operation until the next proof load test.

Very often the initial "fictitious" crack size a_c^p established through the proof load test is much larger than the minimum observable crack size (a_o). Therefore, the service life predicted using the proof load established initial crack size a_c^p could be too conservative and unrealistically short compared with the service life predicted using the minimum observable crack size (a_o) as the initial crack size in the service life calculations.

Sometimes, it might be more convenient to relate the amount of crack growth caused by random load spectrum to the number of equivalent constant-amplitude stress cycles, and then estimate the service life by simply counting the available constant-amplitude stress cycles.

A second-order theory for calculating the service life (number of remaining flights) for a given available crack growth (refs. 1–3) is presented in this report. In addition, a discussion of the previously mentioned equivalent constant-amplitude stress cycling method to estimate the service lives of aerostructural components is also presented.

NOMENCLATURE

A	crack location parameter
a	depth of semielliptic surface crack, in.
a_c^o	operational limit crack size, in.
a_c^p	initial fictitious crack size established by proof load test, in.
a_o	minimum detectable crack size, in.
a_1	crack size at the end of the first flight, in.
C	material constant in Walker crack growth-rate equation, $\frac{\text{in.}}{\text{cycle}}(\text{ksi}\sqrt{\text{in.}})^{-m}$
c	half length of surface crack, in.
E	complete elliptic function of the second kind
F_1	number of remaining flights calculated based on the first-flight data
F_1^*	number of remaining flights calculated from the equivalent constant-amplitude stress cycles method
$\bar{F}_1$	number of remaining flights calculated from the first-order theory
$\tilde{F}_1$	number of remaining flights calculated from the second-order theory
f	fraction of limit load (proof load)
K_{I_C}	mode I critical stress intensity factor, ksi$\sqrt{\text{in.}}$
K_{max}	mode I stress intensity factor associated with σ_{max}
k	modulus of elliptic function
ℓ	number of flights
M_K	flaw magnification factor
m	Walker exponent associated with stress amplitude
N	number of constant-amplitude stress cycles
N_C	maximum number of constant-amplitude stress cycles for service life
N_R	number of random stress cycles
n	Walker exponent associated with stress ratio
Q	surface flaw and plasticity factor
R	stress ratio, $R = \sigma_{min}/\sigma_{max}$
SRB–DTV	solid rocket booster drop test vehicle
V_A	front hook vertical load, lb
V_{BL}	left rear hook vertical load, lb
V_{BR}	right rear hook vertical load, lb
Δa_1	amount of crack growth induced by the first flight, in.
ΔN_ℓ	number of equivalent constant-amplitude stress cycles consumed during the ℓth flight

δa_i	crack growth increment induced by the ith half cycle, in.
σ^*	proof load established stress at the critical stress point, ksi
σ_j	tensile stress at stress point j
σ_{max}	maximum stress of a stress cycle, ksi
σ_{min}	minimum stress of a stress cycle, ksi
σ_s	mean stress (or static stress) of a stress cycle, ksi
σ_U	ultimate stress, ksi
σ_Y	yield stress, ksi
τ	ultimate shear stress, ksi
ϕ	angular coordinate for semielliptic surface crack, rad
$(\,)_i$	quantity associated with ith half stress cycle

SERVICE LIFE

Conventional Method

If Δa_1 is the amount of crack growth induced by the first flight, then the conventional method predicts the number of remaining flights F_1 (service life) based on the following equation (refs. 1–3).

$$F_1 = \frac{a_c^o - a_c^p}{\Delta a_1} \tag{1}$$

where a_c^p and a_c^o are calculated respectively from (refs. 1–3)

$$a_c^p = \frac{Q}{\pi}\left[\frac{K_{I_C}}{AM_K\sigma^*}\right]^2 \tag{2}$$

$$a_c^o = \frac{Q}{\pi}\left[\frac{K_{I_C}}{AM_K f\sigma^*}\right]^2 \tag{3}$$

where σ^* and $f\sigma^*$ ($f < 1$) are respectively, the proof load induced stress (limit stress) and the operational peak stress at the critical stress point; A is the crack location parameter ($A = 1.00$ for the through thickness crack, $A = 1.12$ for both the surface and the edge cracks)(refs. 1–3); M_K is the flaw magnification factor ($M_K = 1.0$ for very shallow surface cracks, $M_K = 1.6$ when the depth of the crack approaches the thickness of the plate); K_{I_C} is the critical stress intensity factor, and Q is the surface flow shape and plasticity factor of a surface crack. If the surface crack is semielliptic in shape, then Q is expressed as (see fig. 1 and refs. 1–3):

$$Q = [E(k)]^2 - 0.212\left(\frac{\sigma^*}{\sigma_Y}\right)^2 \tag{4}$$

where σ_Y is the yield stress, and $E(k)$ is the complete elliptic function of the second kind defined as

$$E(k) = \int_o^{\frac{\pi}{2}} \sqrt{1 - k^2 \sin^2\phi}\, d\phi \tag{5}$$

where ϕ is the angular coordinate for a semielliptic surface crack (see fig. 1) and the modulus k of the elliptic function is defined as

$$k = \sqrt{1 - \left(\frac{a}{c}\right)^2} \tag{6}$$

where a and c are respectively the depth and the half length of a semielliptic surface crack.

Before flight, the actual amount of crack growth Δa_1 (eq. (1)) for the first flight is unknown. The way to estimate Δa_1, before the actual flight, is to perform transient dynamic analysis of the flight vehicle under specified severe maneuvers such as landing, braking, ground turns, flight in severe buffet and turbulence, etc. Actual ground maneuvering of the aircraft can be conducted (for example, taxi runs on straight or curved paths) and generate an actual loading spectrum for each critical component for a short period. Then, the loading spectrum is expanded (extrapolated) to cover the duration of one flight. For large flexible aircraft, such as the B-52 carrier airplane, the ground maneuver could produce a more severe loading spectrum than that of the actual steady flight. If equation (1) predicts a sufficient number of flights available based on Δa_1, calculated from the ground maneuver, one may feel confident to actually conduct one flight to obtain the actual value of Δa_1.

Calculation of Crack Growth

The crack growth caused by the random stress cycling of the first flight may be calculated by using the half-cycle theory (refs. 1–3). The half-cycle theory states that the damage, or crack growth, caused by each half cycle (either increasing or decreasing load) of the random load spectrum is assumed to equal one half of the damage caused by a full cycle of the constant-amplitude load spectrum of the same loading magnitude. Thus, the total damage done by the random load spectrum will be the summation of the microdamages caused by the individual half waves of different loading magnitudes. Figure 3 gives graphical illustrations of the half-cycle theory (refs. 1–3).

Thus, the crack growth Δa_1 caused by the first flight may be calculated as

$$\Delta a_1 = a_1 - a_c^p = \sum_{i=1}^{2N_R} \delta a_i \tag{7}$$

where a_1 is the crack size at the end of the first flight; N_R is the total number of random cycles induced by the first flight; and δa_i is the crack growth increment induced by the ith half cycle, calculated from (refs. 1–3)

$$\delta a_i = \frac{C}{2}\left[(K_{max})_i\right]^m (1 - R_i)^n \tag{8}$$

which is obtained from the Walker equation (refs. 1–3)

$$\frac{da}{dN} = C(K_{max})^m (1 - R)^n \tag{9}$$

by setting $da = \delta a_i, dN = \frac{1}{2}, K_{max} = (K_{max})_i$ and $R = R_i$ for the ith half cycle of random load spectrum. In equations (8) and (9), $C, m,$ and n are the material constants and $(K_{max})_i$ and R_i are, respectively, the maximum stress intensity factor and the stress ratio associated with the ith half cycle and are given by

$$(K_{max})_i = AM_K(\sigma_{max})_i\sqrt{\frac{\pi a_{i-1}}{Q}} \tag{10}$$

$$R_i = \frac{(\sigma_{min})_i}{(\sigma_{max})_i} \tag{11}$$

where $(\sigma_{max})_i$ and $(\sigma_{min})_i$ are respectively, the maximum and the minimum stresses of the ith half cycle (see random stress cycles in fig. 2(a)); a_{i-1} is the crack size at the end of the $(i-1)$th half cycle.

"Minimum-Crack" Method

The proof load established initial crack sizes (a_c^p) are used only for establishing a "baseline" for the aircraft structural component already in service. If the critical stress-point areas can be easily inspected, then the minimum detectable crack size a_o could be used as an initial crack size. Certainly aircraft with zero flight hours can use a_o as an initial crack size with no reliance on proof load requirement.

If the minimum detectable surface crack size a_o (crack depth) turned out to be much smaller than the proof load established intial crack size a_c^p of certain critical structural components (for example, the B-52 hooks which are inspectable) then one can use a_o instead of a_c^p as an initial "fictitious" crack size for the crack growth calculations. Thus, equation (1) may be modified as

$$F_1 = \frac{a_c^o - a_o}{\Delta a_1} \tag{12}$$

where Δa_1 is much smaller than Δa_1 appearing in equation (1) because of smaller initial crack size.

If equation (12) is used in the calculations of service life, the initial crack size a_o for all subsequent flights will remain the same provided interflight crack detection inspection is conducted. Clearly equation (12) will give much longer service life than does equation (1).

SECOND-ORDER THEORY

The conventional equation (eq. (1)) for service life prediction is based on the assumption that the amount of crack growth during each flight for all subsequent flights remains the same as the crack growth Δa_1, caused by the first flight. In reality, the amount of crack growth during each flight will increase steadily with the number of flights accumulated because the initial crack size for the subsequent flight will increase gradually. The new equation for service life prediction will account for the nonuniform crack growth effect. If Δa_ℓ is the amount of crack growth induced by the random load spectrum of the ℓth (ℓ = 1, 2, 3, ...) flight, and if ΔN_ℓ is the number of cycles of an equivalent constant-amplitude load spectrum which also induce a crack growth equal to Δa_ℓ, then the Walker equation (eq. (9)) may be used to relate ΔN_ℓ to Δa_ℓ as

$$\Delta a_\ell = C\left(AM_K\sigma_{max}\sqrt{\frac{\pi}{Q}}\right)^m (1-R)^n (a_{\ell-1})^{\frac{m}{2}}\Delta N_\ell \tag{13}$$

in which the following expression was used

$$K_{max} = AM_K \sigma_{max} \sqrt{\frac{\pi a_{\ell-1}}{Q}} \tag{14}$$

where $a_{\ell-1}$ is the crack size at the end of the $(\ell-1)$th flight.

For simplicity, if we assume that the equivalent constant-amplitude load spectra for all flights are identical (that is, σ_{max}, R, and ΔN_ℓ remain the same), then equation (13) could be used to establish the following crack growth ratios and expand them in terms of $\frac{\Delta a_1}{a_c^p}$ up to second-order terms assuming that $\frac{\Delta a_1}{a_c^p}$ is small (i.e., $\frac{\Delta a_1}{a_c^p} \ll 1$):

$$\frac{\Delta a_1}{\Delta a_1} = \left(\frac{a_c^p}{a_c^p}\right)^{\frac{m}{2}} = 1 \tag{15}$$

$$\begin{aligned} \frac{\Delta a_2}{\Delta a_1} &= \left(\frac{a_1}{a_c^p}\right)^{\frac{m}{2}} = \left(\frac{a_c^p + \Delta a_1}{a_c^p}\right)^{\frac{m}{2}} \\ &= 1 + 1\left(\frac{m}{2}\frac{\Delta a_1}{a_c^p}\right)\left[1 - \frac{1}{2}\left(\frac{m}{2}\frac{\Delta a_1}{a_c^p}\right)\right] + 1^2\left(1 - \frac{1}{m}\right)\left(\frac{m}{2}\frac{\Delta a_1}{a_c^p}\right)^2 + \ldots \end{aligned} \tag{16}$$

$$\begin{aligned} \frac{\Delta a_3}{\Delta a_1} &= \left(\frac{a_2}{a_c^p}\right)^{\frac{m}{2}} = \left(\frac{a_c^p + \Delta a_1 + \Delta a_2}{a_c^p}\right)^{\frac{m}{2}} \\ &= 1 + 2\left(\frac{m}{2}\frac{\Delta a_1}{a_c^p}\right)\left[1 - \frac{1}{2}\left(\frac{m}{2}\frac{\Delta a_1}{a_c^p}\right)\right] + 2^2\left(1 - \frac{1}{m}\right)\left(\frac{m}{2}\frac{\Delta a_1}{a_c^p}\right)^2 + \ldots \end{aligned} \tag{17}$$

$$\begin{aligned} \frac{\Delta a_4}{\Delta a_1} &= \left(\frac{a_3}{a_c^p}\right)^{\frac{m}{2}} = \left(\frac{a_c^p + \Delta a_1 + \Delta a_2 + \Delta a_3}{a_c^p}\right)^{\frac{m}{2}} \\ &= 1 + 3\left(\frac{m}{2}\frac{\Delta a_1}{a_c^p}\right)\left[1 - \frac{1}{2}\left(\frac{m}{2}\frac{\Delta a_1}{a_c^p}\right)\right] + 3^2\left(1 - \frac{1}{m}\right)\left(\frac{m}{2}\frac{\Delta a_1}{a_c^p}\right)^2 + \ldots \end{aligned} \tag{18}$$

$$\vdots$$

$$\begin{aligned} \frac{\Delta a_\ell}{\Delta a_1} &= \left(\frac{a_{\ell-1}}{a_c^p}\right)^{\frac{m}{2}} = \left(\frac{a_c^p + \Delta a_1 + \Delta a_2 + \Delta a_3 + \ldots \Delta a_{\ell-1}}{a_c^p}\right)^{\frac{m}{2}} \\ &= 1 + (\ell-1)\left(\frac{m}{2}\frac{\Delta a_1}{a_c^p}\right)\left[1 - \frac{1}{2}\left(\frac{m}{2}\frac{\Delta a_1}{a_c^p}\right)\right] + (\ell-1)^2\left(1 - \frac{1}{m}\right)\left(\frac{m}{2}\frac{\Delta a_1}{a_c^p}\right)^2 + \ldots \end{aligned} \tag{19}$$

$$\vdots$$

If the available crack growth $a_c^o - a_c^p$ can allow $\tilde{F}_1$ number of flights, then one can write:

$$\frac{a_c^o - a_c^p}{\Delta a_1} = \frac{\overbrace{\Delta a_1 + \Delta a_2 + \Delta a_3 + \ldots + \Delta a_\ell + \ldots \Delta a_{\tilde{F}_1}}^{\tilde{F}_1\ terms}}{\Delta a_1} \tag{20}$$

where the left-hand side of this equation is F_1 according to equation (1).

Substitution of equations (15)–(19) into equation (20) yields:

$$\begin{aligned} F_1 &= \overbrace{1+1+1+1+\ldots+1}^{\tilde{F}_1\ terms} \\ &+ \left[0 + \overbrace{1+2+3+\ldots+(\ell-1)+\ldots+(\tilde{F}_1-1)}^{(\tilde{F}_1-1)\ terms} \right] \left(\frac{m}{2}\frac{\Delta a_1}{a_c^p}\right)\left[1 - \frac{1}{2}\left(\frac{m}{2}\frac{\Delta a_1}{a_c^p}\right)\right] \\ &+ \left[0^2 + \overbrace{1^2+2^2+3^2+\ldots+(\ell-1)^2+\ldots+(\tilde{F}_1-1)^2}^{(\tilde{F}_1-1)\ terms} \right] \left(1-\frac{1}{m}\right)\left(\frac{m}{2}\frac{\Delta a_1}{a_c^p}\right)^2 + \ldots \end{aligned} \tag{21}$$

which becomes, after summations of numbers:

$$\begin{aligned} F_1 = \tilde{F}_1 &+ \frac{1}{2}\tilde{F}_1(\tilde{F}-1)\left(\frac{m}{2}\frac{\Delta a_1}{a_c^p}\right)\left[1-\frac{1}{2}\left(\frac{m}{2}\frac{\Delta a_1}{a_c^p}\right)\right] \\ &+ \frac{1}{3}\tilde{F}_1(\tilde{F}_1-1)\left(\tilde{F}_1-\frac{1}{2}\right)\left(1-\frac{1}{m}\right)\left(\frac{m}{2}\frac{\Delta a_1}{a_c^p}\right)^2 + \ldots \end{aligned} \tag{22}$$

After grouping terms and rearrangement, equation (22) may be written in the following standard form of cubic equation:

$$\tilde{F}_1{}^3 + p\tilde{F}_1{}^2 + q\tilde{F}_1 + r \approx 0 \tag{23}$$

where

$$p \equiv \frac{3}{2(m-1)}\left(1 - \frac{3}{2}m + 2\frac{a_c^p}{\Delta a_1}\right) \tag{24}$$

$$q \equiv \frac{1}{2}\left\{1 + \frac{3}{m-1}\left[\frac{m}{2} - 2\frac{a_c^p}{\Delta a_1} + \frac{8}{m}\left(\frac{a_c^p}{\Delta a_1}\right)^2\right]\right\} \tag{25}$$

$$r \equiv -\frac{12F_1}{m(m-1)}\left(\frac{a_c^p}{\Delta a_1}\right)^2 \tag{26}$$

The real root of equation (23) is then given by

$$\tilde{F}_1 = B + D - \frac{p}{3} \tag{27}$$

where

$$\left.\begin{matrix}B\\D\end{matrix}\right\} = \sqrt[3]{-\frac{\beta}{2} \pm \sqrt{\frac{\beta^2}{4} + \frac{\alpha^3}{27}}} \tag{28}$$

where

$$\alpha \equiv \frac{1}{3}(3q - p^2) \tag{29}$$

$$\beta \equiv \frac{1}{27}(2p^3 - 9pq + 27r) \tag{30}$$

In equation (21), if the second-order terms are neglected, then the number of flights $\bar{F}_1$ predicted based on the first-order expansion will be

$$\bar{F}_1 = \frac{2a_c^p}{m\Delta a_1}\left(\sqrt{1 + \frac{m\Delta a_1}{a_c^p}F_1} - 1\right) \tag{31}$$

which has already been published in references 1 and 2.

EQUIVALENT CONSTANT-AMPLITUDE STRESS CYCLES

In this section, we attempt to consider the crack growth Δa_1, (see eq. (7)) caused by random stress cycling as if it were caused by equivalent constant-amplitude stress cycling (see fig. 2(b)). If the constant-amplitude load spectrum is cycling about the mean (static) stress σ_s, then the maximum stress σ_{max} and the minimum stress σ_{min} of the equivalent constant-amplitude stress cycle is related through

$$\sigma_{min} = 2\sigma_s - \sigma_{max} \tag{32}$$

If σ_{max} is a fraction of the limit stress σ^* (proof load induced stress), namely,

$$\sigma_{max} = f\sigma^*; \qquad f < 1 \tag{33}$$

then one can write

$$K_{max} = AM_K f\sigma^*\sqrt{\frac{\pi a}{Q}} \tag{34}$$

$$R = \frac{\sigma_{min}}{\sigma_{max}} = \frac{2\sigma_s}{f\sigma^*} - 1 \tag{35}$$

If the initial crack size is a_c^p, then the number of the equivalent constant-amplitude stress cycles, N, required to extend the initial crack size a_c^p up to an arbitrary size "a" could be obtained by integrating equation (9) as

$$N = \frac{a^{1-\frac{m}{2}} - (a_c^p)^{1-\frac{m}{2}}}{\left(1-\frac{m}{2}\right)C\left[AM_K f\sigma^*\sqrt{\frac{\pi}{Q}}\right]^m\left[2\left(1-\frac{\sigma_s}{f\sigma^*}\right)\right]^n} \tag{36}$$

From equation (36), the number of equivalent constant-amplitude stress cycles N_C available for operation, and the number of equivalent constant-amplitude stress cycles consumed by the first flight, N_1, to cause the same damage Δa_1 as does the random stress cycling, may be obtained by setting $a = a_c^o$ and $a = a_1$ respectively.

If every flight after the first flight consumes the same number of equivalent constant-amplitude stress cycles as does the first flight, then the service life F_1^* may be calculated from

$$F_1^* = \frac{N_C}{N_1} = \frac{(a_c^o)^{1-\frac{m}{2}} - (a_c^p)^{1-\frac{m}{2}}}{a_1^{1-\frac{m}{2}} - (a_c^p)^{1-\frac{m}{2}}} \tag{37}$$

where equation (36) is used, and $a_1 = a_c^p + \Delta a_1$ is to be calculated from equation (7).

When the random load spectrum is converted into an equivalent constant-amplitude load spectrum, for service life estimates one can merely count the number of the equivalent constant-amplitude stress cycles. If N_1 is consumed for the first flight, then N_1 is used to calculate the remaining flights (eq. (37)) with accuracy, because the amount of the equivalent constant-amplitude stress cycles consumed for each of the subsequent flights is theoretically identical.

NUMERICAL EXAMPLE

The numerical example chosen for the calculations of service life of aerospace structural components is the NASA B-52 carrier aircraft air-launching system (pylon) hooks as shown in figures 4 and 5. Figure 5 also shows the locations of the critical stress points and the stress–hook-load relationships determined from stress analysis (ref. 4). Through one front hook and two rear hooks of the pylon of the B-52 aircraft, a winged Pegasus® rocket (approximately 44,629 lb) will be carried to high altitude (approximately 40,000 ft) to release it for firing into orbit. The B-52 aircraft was used earlier to carry heavy stores such as the X-15 air-launched rocket plane (57,250 lb) and the space shuttle solid rocket booster drop test vehicle (SRB–DTV, 49,000 lb). The data accumulated for those vehicles may be used to estimate the "preflight" service lives of the three hooks when the store is the Pegasus rocket, because of weight proximity.

Input Numerical Values

Assuming that the surface cracks (initial and after growth) are semicircular in shape (that is, $\frac{a}{2c} = \frac{1}{2}$), and that the stress level at the critical stress point of each hook reached the yield point (the hooks are designed to carry yielding zones), then from figure 1 one obtains Q = 2.265 for $\frac{a}{2c} = \frac{1}{2}$. In the crack growth calculations A = 1.12 and M_K = 1.0 were used. Other numerical values used in the crack growth calculations are given in table 1.

® Pegasus is a registered trademark of Orbital Sciences Corp., Fairfax, Virginia.

Table 1. Material properties for B-52 pylon hooks.

Part name	Material	σ_U, ksi	σ_Y, ksi	τ, ksi	K_{I_C}, ksi $\sqrt{\text{in.}}$	C, $\frac{\text{in.}}{\text{cycle}}$ (ksi $\sqrt{\text{in.}}$)$^{-m}$	m	n
Front hook	Inconel 718® alloy	175	145	135	125	9.220×10^{-12}	3.60	2.16
Left rear hook	AMAX MP35N* alloy	250	235	141	124	2.944×10^{-11}	3.24	1.69
Right rear hook	AMAX MP35N* alloy	250	235	141	124	2.944×10^{-11}	3.24	1.69

® Inconel 718 is a registered trademark of Huntington Alloy Products Division, International Nickel Company, Huntington, West Virginia.
*AMAX MP35N is a trademark of SPS Technologies, Inc., Jenkintown, Pennsylvania.

Using the numerical values given in table 1, and the proof hook loads V_A = 36,500 lb, $V_{BL} = V_{BR}$ = 57,819 lb, the initial crack sizes a_c^p and the operational limit crack sizes a_c^o (for $f = 0.6$) may be calculated respectively from equations (2) and (3) as:

Table 2. Proof and operational limit crack sizes.

Part name	Proof hook load, lb	a_c^p, in.	a_c^o, in.($f = 0.6$)*	$\frac{\Delta a_1}{a_c^p}$ ($f = 0.6$)*
Front hook, V_A	36,500	0.1247	0.3465	0.01814
Left rear hook, V_{BL}	57,819	0.0774	0.2151	0.00761
Right rear hook, V_{BR}	57,819	0.0774	0.2151	0.00761

*f = 0.6 was the average operational peak load level for the case of SRB–DTV.

The present-day crack detection techniques could detect a surface crack approximately 0.02 in. long. Thus, if the surface crack is semicircular in shape, then the minimum detectable crack depth is approximately 0.01 in. Clearly, this value is far less than the proof load established initial crack sizes listed in table 2. In the service life calculation using the "Minimum-Crack" method, the initial crack size a_o will be taken as a_o = 0.01 in.

Crack Growth Ratios

Figure 6 shows crack growth ratio $\frac{\Delta a_\ell}{\Delta a_1}$ plotted as a function of the number of flights ℓ for the front hook using the first- and the second-order theories. The first-order theory (eq. (31)) gives linear increase of $\frac{\Delta a_\ell}{\Delta a_1}$ with increasing ℓ. However, the second-order theory (eq. (23)) gives nonlinear curve with lower values of $\frac{\Delta a_\ell}{\Delta a_1}$ in the region $1 < \ell < 41$, beyond that the second-order theory predicts much higher values of $\frac{\Delta a_\ell}{\Delta a_1}$ than the first-order theory. The conventional theory gives a simple horizontal line $\frac{\Delta a_\ell}{\Delta a_1} = 1$.

Figure 7 shows similar plots for the rear hook. Unlike the front hook, the second-order curve does not intersect with the first-order curve until $\ell \approx 120$ because of different values of m and $\frac{\Delta a_1}{a_c^p}$.

Remaining Flights

Table 3 lists the numbers of remaining flights $\bar{F}_1$ and $\tilde{F}_1$, for the front and rear hooks, calculated respectively from the first- and the second-order theories, compared with the corresponding number of flights F_1 based on the conventional method (assuming equal amount of crack growth for all subsequent flights (ref. 1)). It is clear that the conventional theory exceedingly overpredicts the predicted service life. Values in table 3 are plotted in figures 8 and 9 respectively for the front and rear hooks for easy visualization of the curves for F_1, $\bar{F}_1$, and $\tilde{F}_1$.

Table 3. Number of remaining flights calculated from first- and second-order theories compared to the conventional method.

	Front hook		Rear hook	
F_1	$\bar{F}_1$	$\tilde{F}_1$	$\bar{F}_1$	$\tilde{F}_1$
1	1	1	1	1
50	33	30	40	39
100	53	45	70	65
150	70	56	95	85
200	84	65	116	101
250	97	72	136	116
300	108	79	154	128
350	119	85	171	139
400	129	90	186	149
450	138	95	201	159
500	147	99	215	167
550	155	103	228	175
600	164	107	241	183
650	171	111	254	190
700	179	114	265	197
750	186	118	277	204
800	193	121	288	210
850	200	124	299	216
900	206	127	310	222
950	213	130	320	227
1000	219	132	330	233

For the given values of m and $\frac{\Delta a_1}{a_c^p}$ for the B-52 front and rear hooks (tables 1 and 2), the predicted service life for the two hooks based on the conventional theory and the first- and the second-order theories are presented in table 4:

Table 4. B-52 hooks service lives based on conventional, first- and second-order theories.

	F_1	$\bar{F}_1$	$\tilde{F}_1$
Front hook	98	52	45
Rear hook	234	130	110

Clearly the conventional theory gives too optimistic a service life prediction. The service life of the front hook is somewhat shorter than that of the rear hook.

Figures 10 and 11 show the crack growth curves for the front and rear hooks, respectively, based on the equivalent constant-amplitude stress cycle method. In each figure, the upper curve is the plot of equation (37) (that is, initial crack size is the proof load established crack size a_c^p). The lower curve is the plot of equation (37) with a_c^p replaced with a_o as an initial crack size. Using a_o as an initial crack size instead of a_c^p, the service lives of the hooks are greatly enhanced. Table 5 summarizes the results of the equivalent constant-amplitude stress cycle method. Predictions from the conventional theory are also shown for comparison.

Table 5. B-52 hooks service lives based on the equivalent constant-amplitude stress cycles method, ($f = 0.6$).

	Initial crack size						
	a_c^p	a_o	a_c^p	a_o	a_c^p	a_o	a_c^p
	Stress cycles				Remaining flights		
	N_1		N_C		F_1^*		F_1
Front hook	67.08	67.08	2623	3329	39	496	98
Rear hook	14.88	14.88	1490	9602	100	645	234

Notice that the number of equivalent constant-amplitude stress cycles for cycling at 60 percent ($f = 0.6$) of limit stress consumed during each flight (N_1) are relatively low and are independent of the initial crack size. For the initial crack size of a_c^p, the equivalent constant-amplitude stress cycles method predicts the most conservative service life as compared with other theories (tables 4 and 5).

Accuracies of Expansions

To check the accuracies of the first- and the second-order theories, values of the crack growth rate $\frac{\Delta a_2}{\Delta a_1}$ (eq. (16)) were calculated from the exact expression for $\frac{\Delta a_2}{\Delta a_1}$ (before expansion of eq. (16)), and from the first- and the second-order expansions (eq. (16)). The results are tabulated in table 6.

Table 6. Accuracy of expansion for $\frac{\Delta a_2}{\Delta a_1}$.

$\frac{\Delta a_2}{\Delta a_1}$	Front hook	Rear hook
Exact expression $\left(1 + \frac{\Delta a_1}{a_c^p}\right)^{\frac{m}{2}}$	1.032887789	1.012357255
First-order expansion $1 + \frac{m}{2}\frac{\Delta a_1}{a_c^p}$	$\boxed{1.032}^{*}651163$	$\boxed{1.0123}^{*}28200$
Second-order expansion (eq. (16))	$\boxed{1.03288}^{*}8074$	$\boxed{1.0123572}^{*}82$

$^{*}\boxed{}$ accurate digits

This table shows that the second-order expansion gives very accurate values for $\frac{\Delta a_2}{\Delta a_1}$, thus, the service life predicted from the second-order theory is quite reliable.

CONCLUDING REMARKS

The second-order theory for predicting the service life of aerospace structural components was presented. The service life predicted from the second-order theory was compared with those predicted from the previously developed first-order theory and the conventional method (constant amount of crack growth for all subsequent flights) of service life predictions. The second-order theory (based on the second-order expansion of the crack growth rate) could give reasonably accurate values of crack growth rate compared with the exact values.

The new equivalent constant-amplitude stress cycles method was proposed. This method gave the most conservative service life predictions. The use of minimum detectable crack size, instead of proof load established crack size as an initial crack size, could give a more realistically longer service life.

Dryden Flight Research Facility
National Aeronautics and Space Administration
Edwards, California, August 18, 1991

REFERENCES

1. Ko, W.L., A.L. Carter, W.W. Totton, and J.M. Ficke, *Application of Fracture Mechanics and Half-Cycle Method to the Prediction of Fatique Life of B-52 Aircraft Pylon Components*, NASA TM-88277, 1989.

2. Ko, William L., *Prediction of Service Life of Aircraft Structural Components Using the Half-Cycle Method*, NASA TM-86812, 1987.

3. Ko, W.L., "Application of Fracture Mechanics and Half-Cycle Theory to the Prediction of Fatique Life of Aerospace Structural Components," *International Journal of Fracture*, vol. 39, Mar. 1989, pp. 45–62.

4. Ko, William L., and Lawrence S. Schuster, *Stress Analyses of B-52 Pylon Hooks*, NASA TM-84924, 1985.

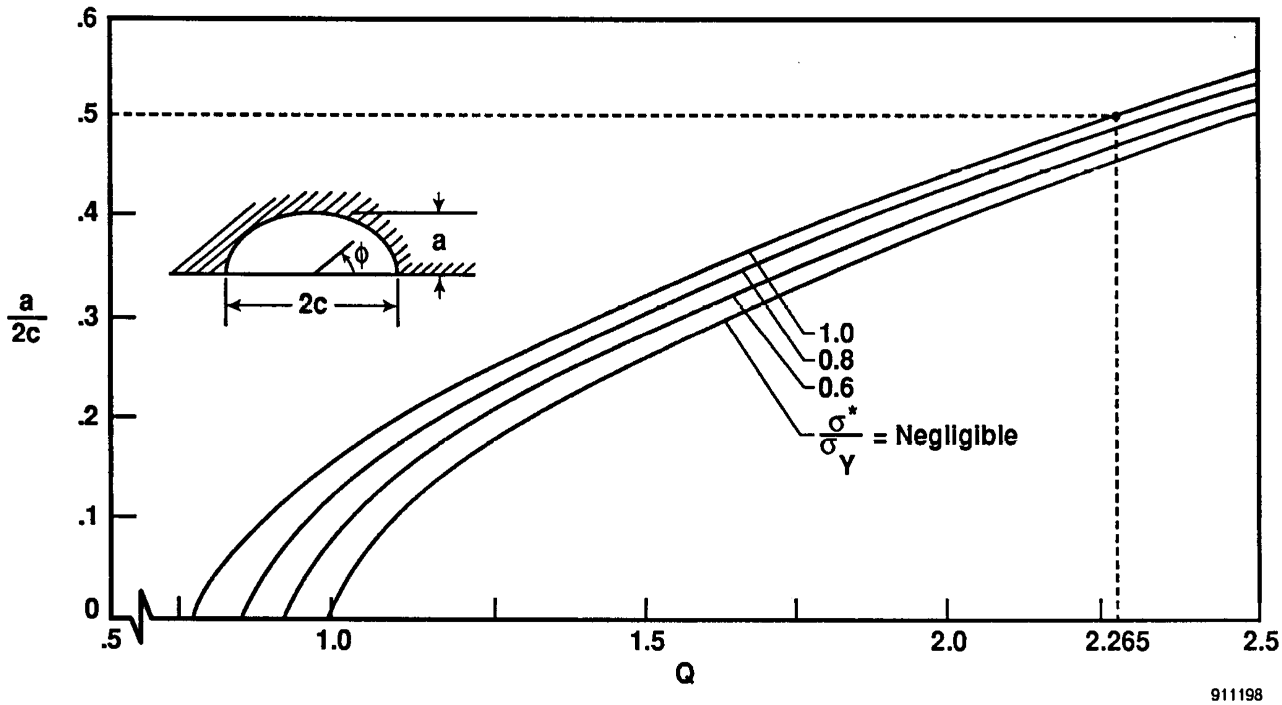

Figure 1. Surface flaw shape and plasticity factor for semielliptic surface crack.

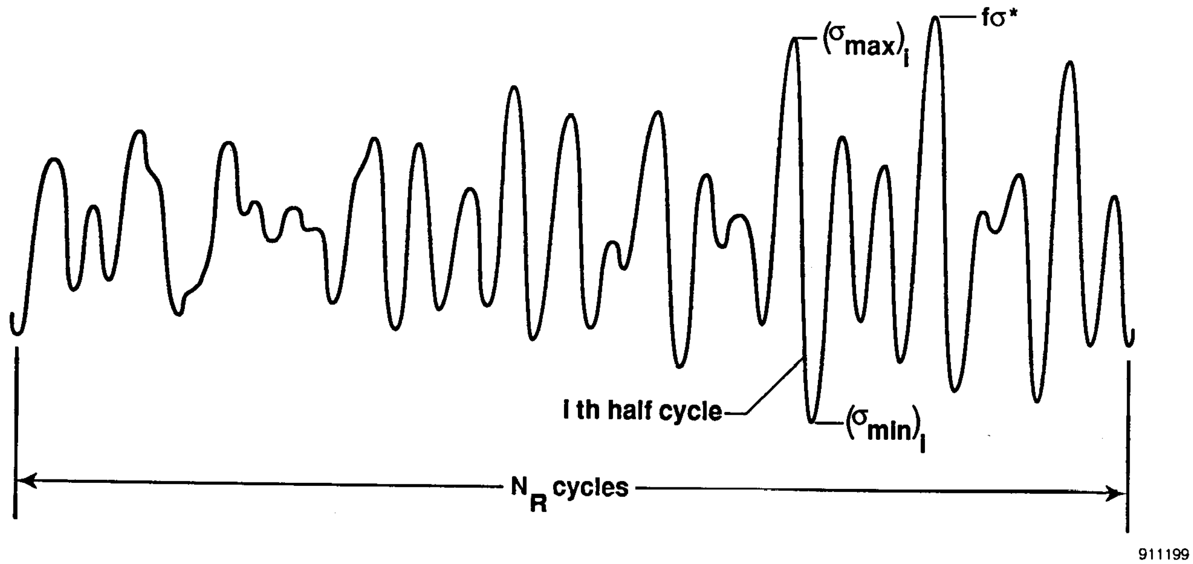

(a) Random stress cycles.

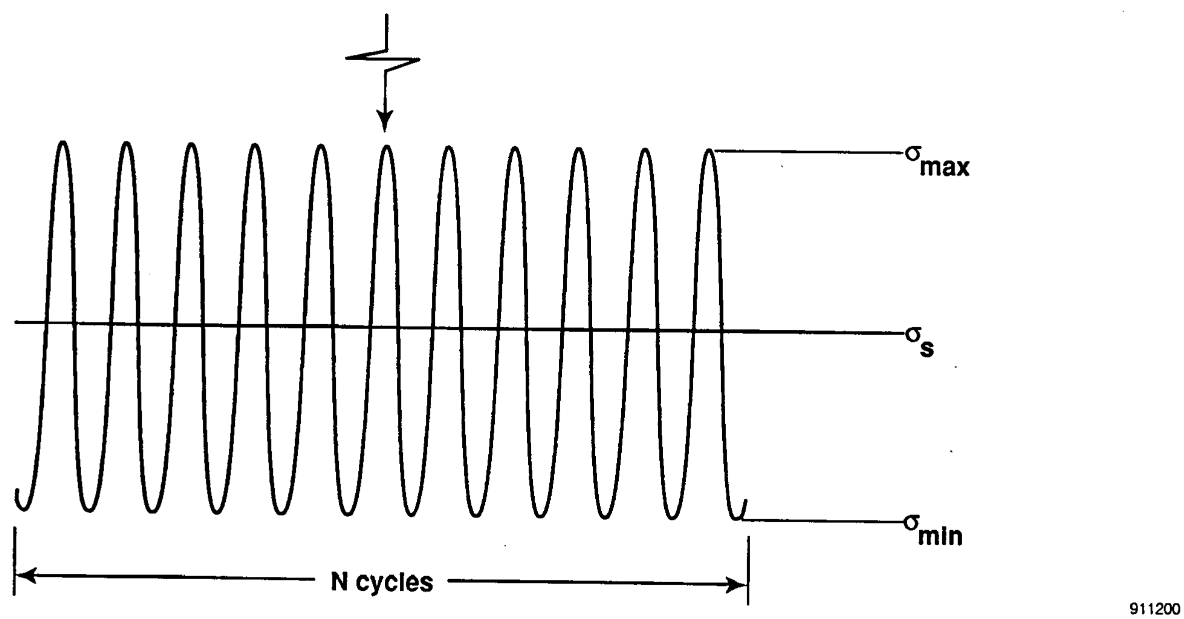

(b) Constant-amplitude stress cycles.

Figure 2. Random stress cycles and equivalent constant-amplitude stress cycles.

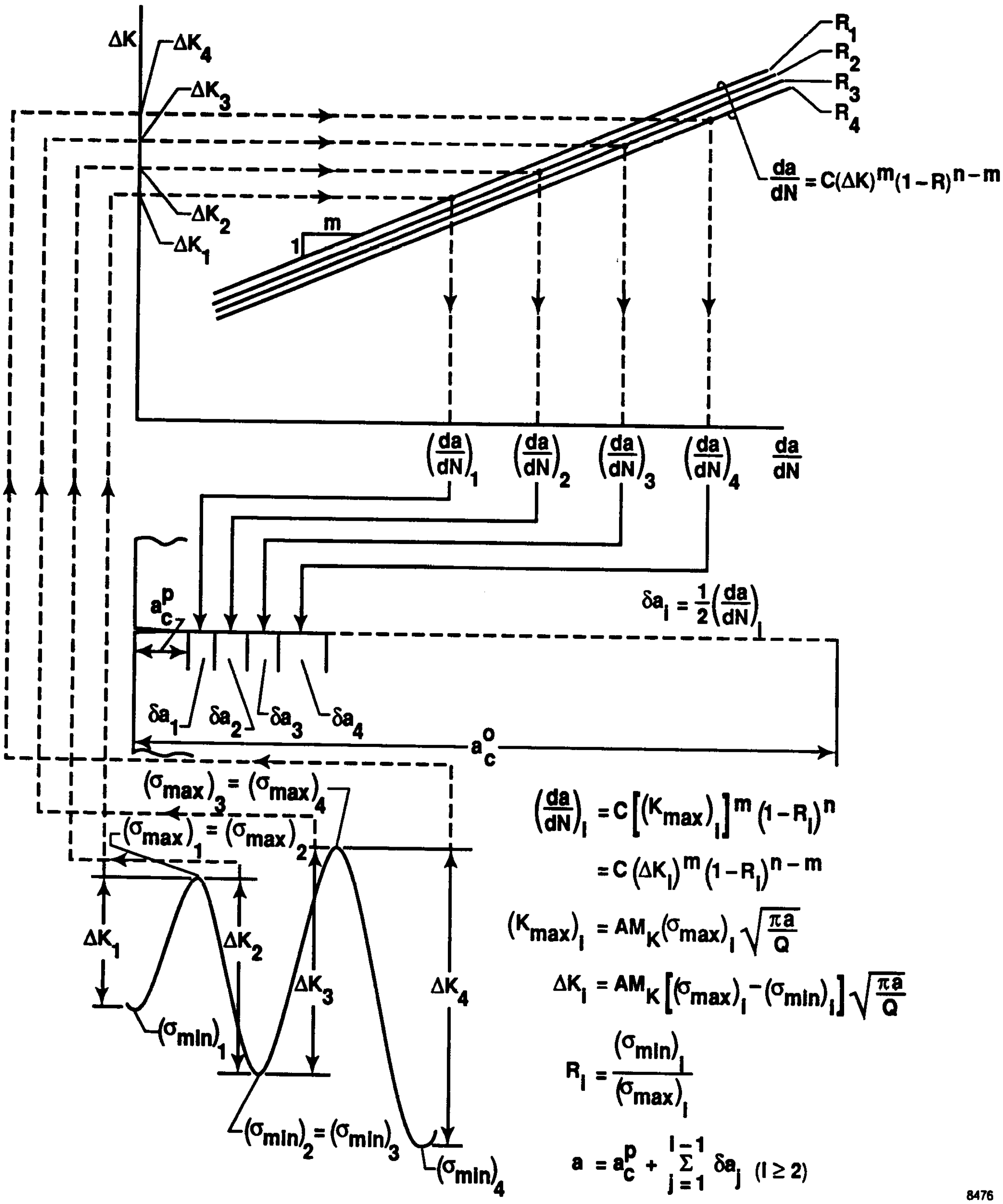

Figure 3. Graphic evaluation of crack increments for random stress cycles using half-cycle method.

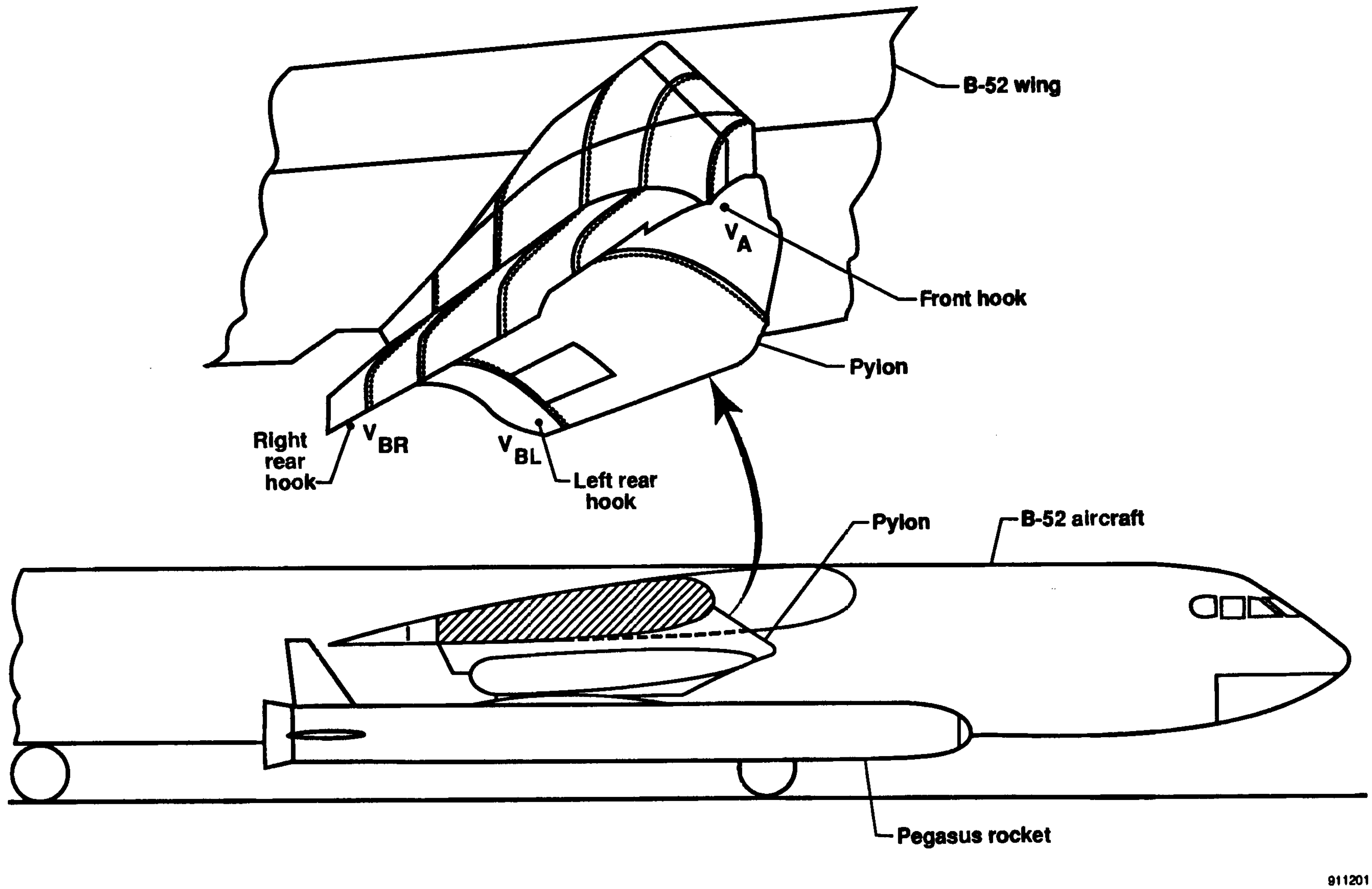

Figure 4. B-52 aircraft pylon carrying winged Pegasus rocket.

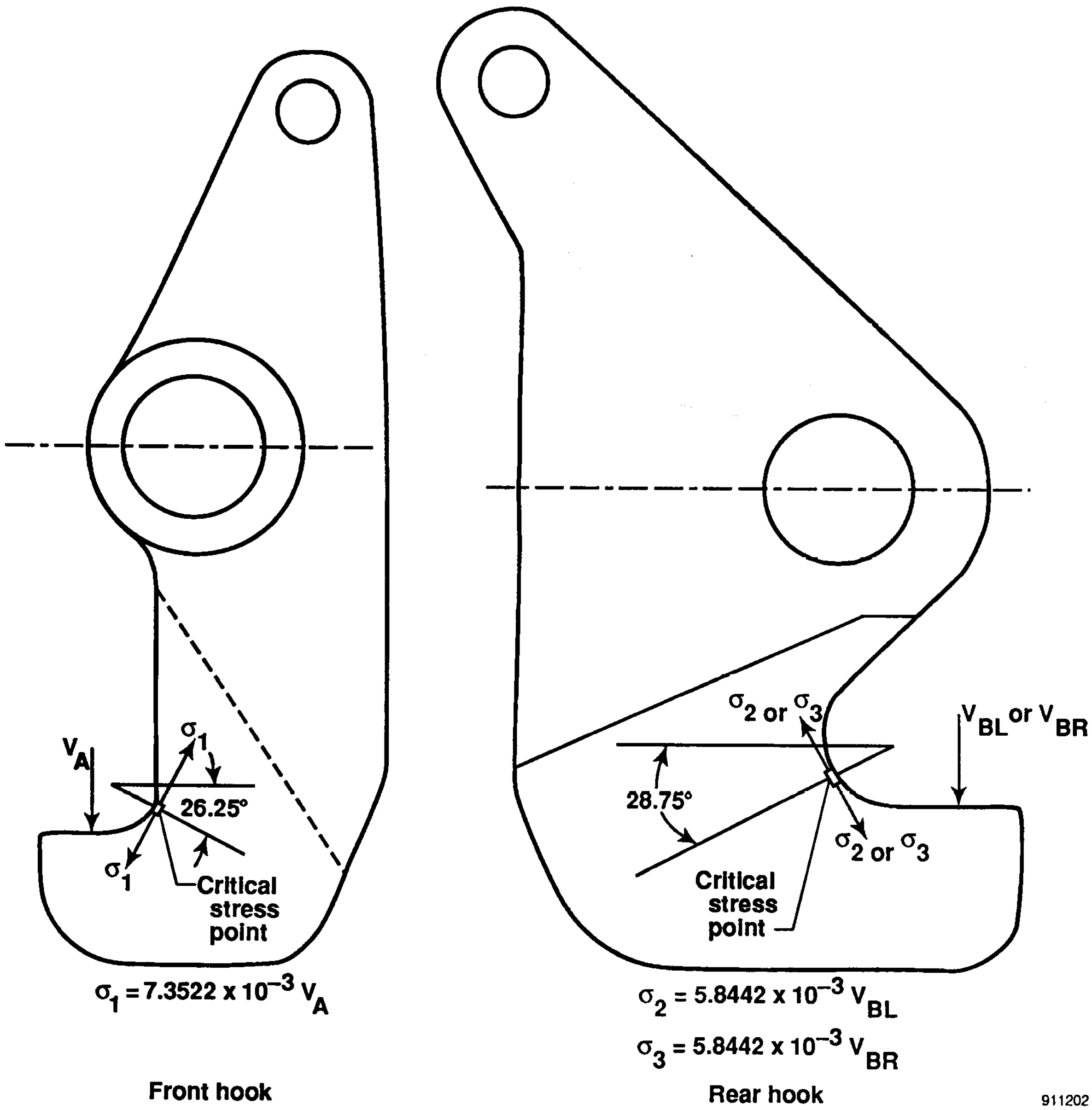

Figure 5. Critical stress points in B-52 pylon front and rear hooks.

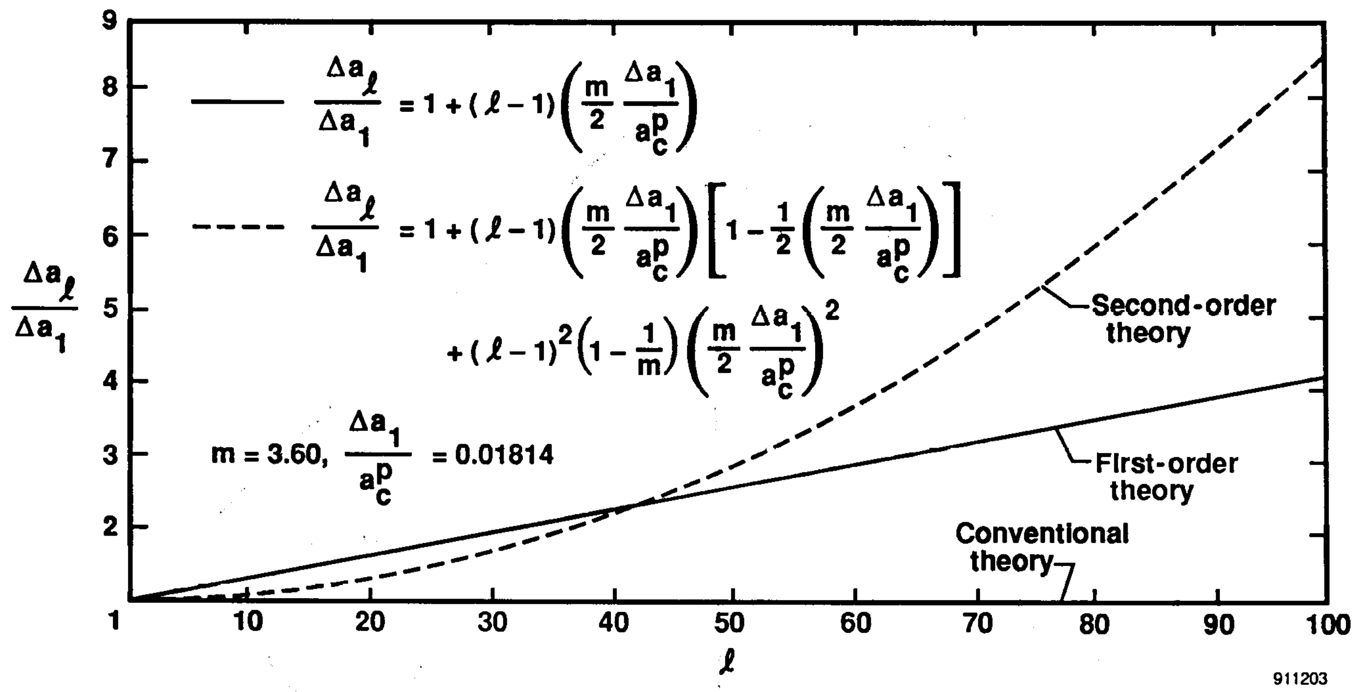

Figure 6. Crack growth ratio as a function of number of flights based on the first- and second-order theories; front hook.

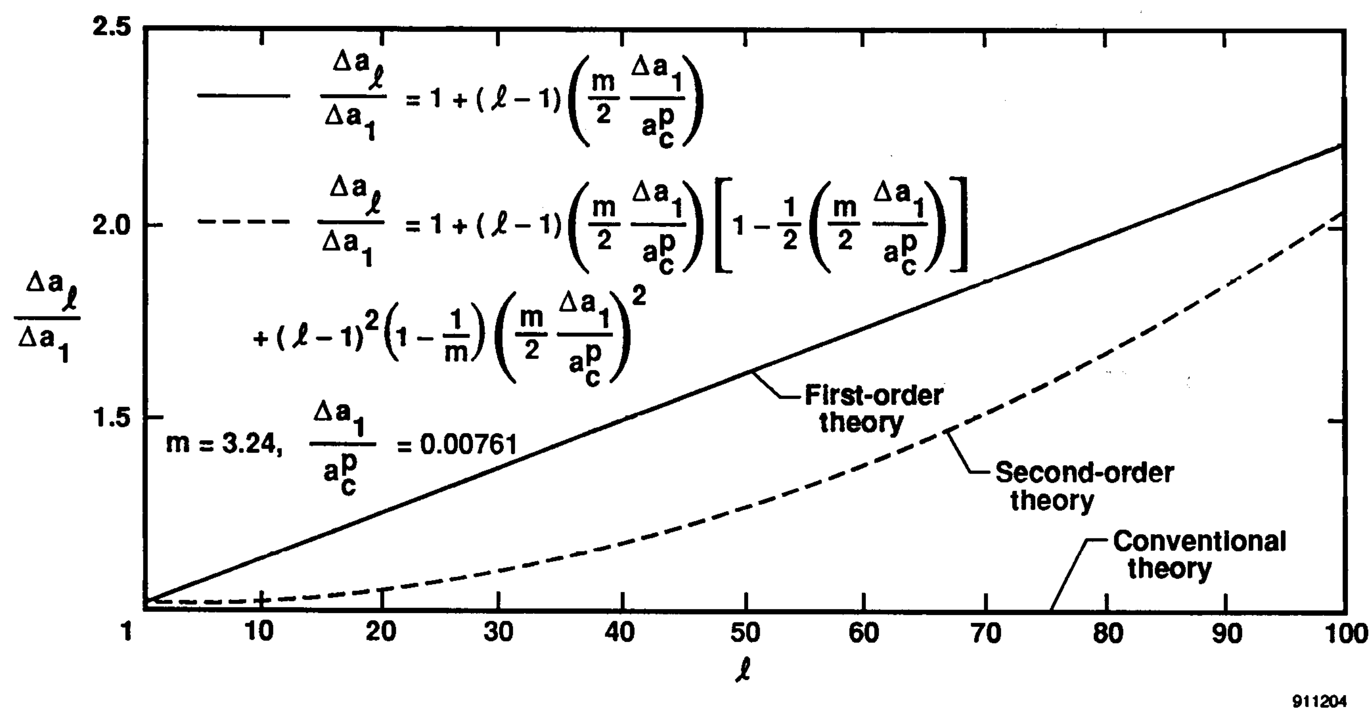

Figure 7. Crack growth ratio as a function of number of flights based on the first- and second-order theories; rear hook.

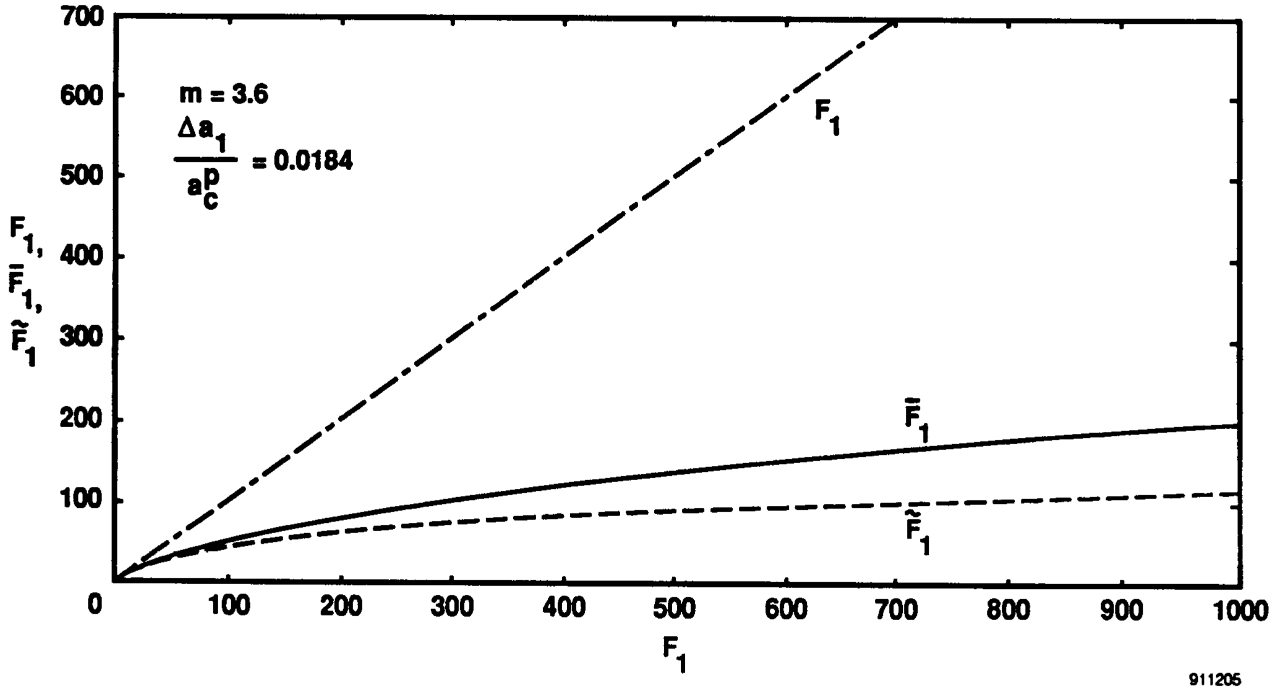

Figure 8. Comparison of number of remaining flights predicted from conventional theory and the first- and second-order theories; front hook.

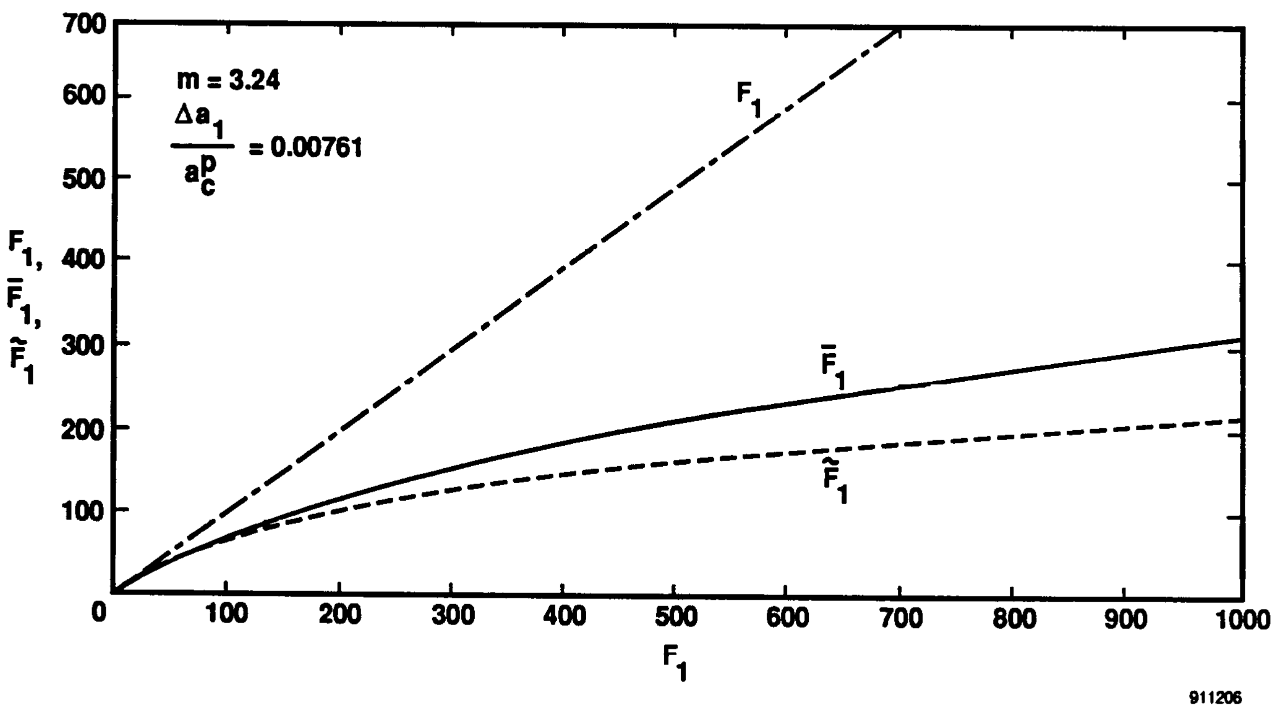

Figure 9. Comparison of number of remaining flights predicted from conventional theory and the first- and second-order theories; rear hook.

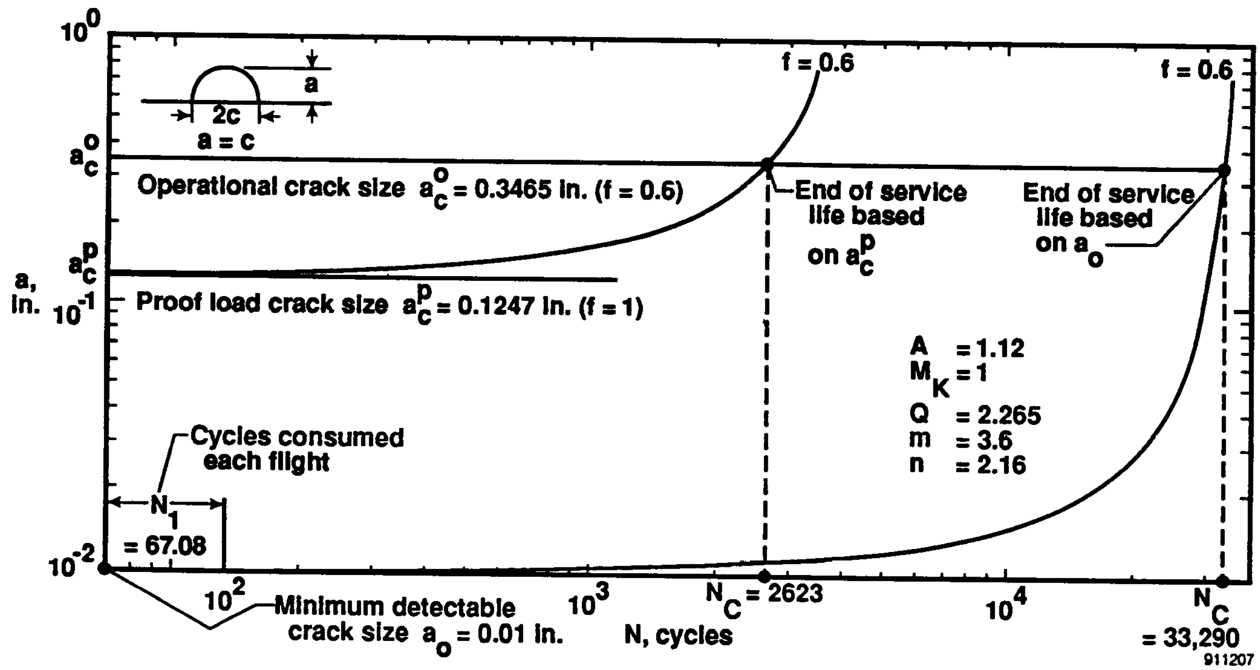

Figure 10. Comparison of service lives of front hook based on different initial crack sizes.

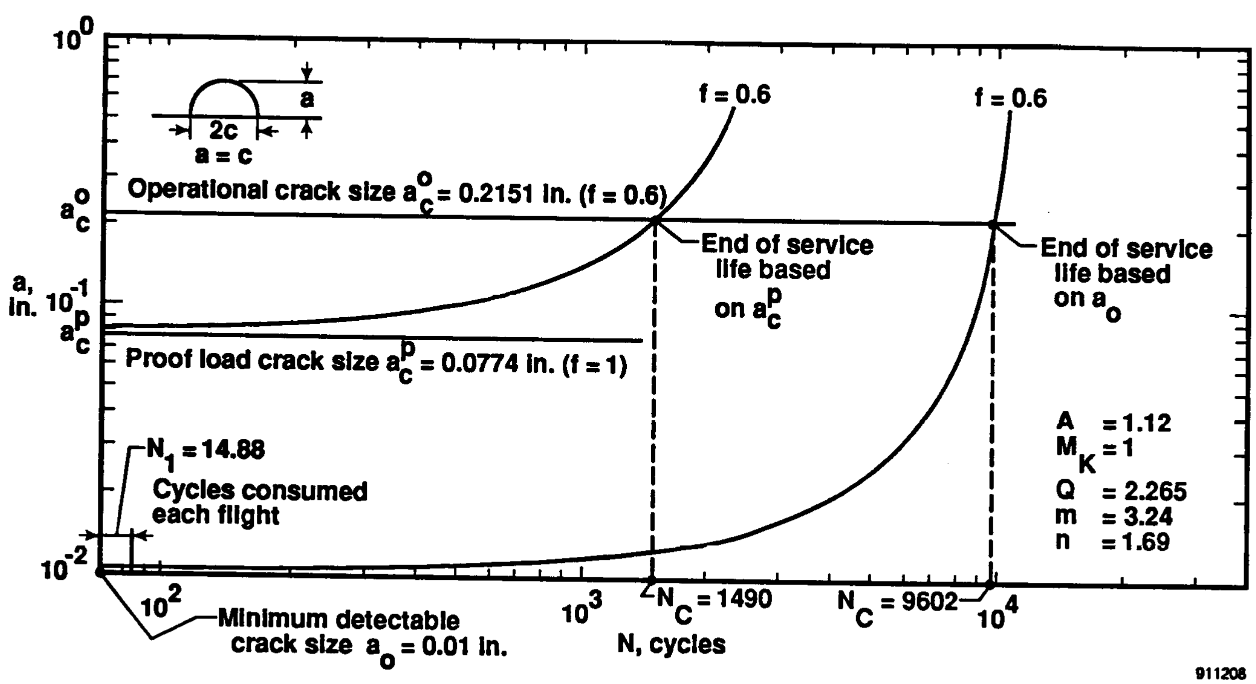

Figure 11. Comparison of service lives of rear hook based on different initial crack sizes.

REPORT DOCUMENTATION PAGE	Form Approved OMB No. 0704-0188

1. AGENCY USE ONLY *(Leave blank)*

2. REPORT DATE
March 1992

3. REPORT TYPE AND DATES COVERED
Technical Memorandum

4. TITLE AND SUBTITLE
Practical Theories for Service Life Prediction of Critical Aerospace Structural Components

5. FUNDING NUMBERS
WU 505-63-40

6. AUTHOR(S)
William L. Ko, Richard C. Monaghan, and Raymond H. Jackson

7. PERFORMING ORGANIZATION NAME(S) AND ADDRESS(ES)
NASA Dryden Flight Research Facility
P.O. Box 273
Edwards, California 93523-0273

8. PERFORMING ORGANIZATION REPORT NUMBER
H-1760

9. SPONSORING/MONITORING AGENCY NAME(S) AND ADDRESS(ES)
National Aeronautics and Space Administration
Washington, DC 20546-0001

10. SPONSORING/MONITORING AGENCY REPORT NUMBER
NASA TM-4354

11. SUPPLEMENTARY NOTES

12a. DISTRIBUTION/AVAILABILITY STATEMENT
Unclassified — Unlimited
Subject Category 39

12b. DISTRIBUTION CODE

13. ABSTRACT *(Maximum 200 words)*

A new second-order theory was developed for predicting the service lives of aerospace structural components. The predictions based on this new theory were compared with those based on the Ko first-order theory and the classical theory of service life predictions. The new theory gives very accurate service life predictions. An equivalent constant-amplitude stress cycles method was proposed for representing the random load spectrum for crack growth calculations. This method predicts the most conservative service life. The proposed use of minimum detectable crack size, instead of proof load established crack size as an initial crack size for crack growth calculations, could give more a realistic service life.

14. SUBJECT TERMS
Fracture mechanics; Half-cycle theory; Random stress cycles; Service life prediction

15. NUMBER OF PAGES
28

16. PRICE CODE
A03

17. SECURITY CLASSIFICATION OF REPORT	18. SECURITY CLASSIFICATION OF THIS PAGE	19. SECURITY CLASSIFICATION OF ABSTRACT	20. LIMITATION OF ABSTRACT
Unclassified	Unclassified		

NSN 7540-01-280-5500

Standard Form 298 (Rev. 2-89)
Prescribed by ANSI Std. Z39-18
298-102

NASA-Langley, 1992